Journal of Electron Spectroscopy and Related Phenomena 196 (2014) 136–141

Contents lists available at ScienceDirect

Journal of Electron Spectroscopy and Related Phenomena

journal homepage: www.elsevier.com/locate/elspec

Strongly correlated transition metal compounds investigated by soft X-ray spectroscopies and multiplet calculations

J. Jiménez-Mier[a,*], P. Olalde-Velasco[a,b], G. Herrera-Pérez[a], G. Carabalí -Sandoval[a], E. Chavira[c], W.-L. Yang[b], J. Denlinger[b]

[a] Instituto de Ciencias Nucleares, UNAM, 04510 México, DF, Mexico
[b] The Advanced Light Source, Lawrence Berkeley Laboratory, Berkeley, CA 94720, USA
[c] Instituto de Investigaciones en Materiales, UNAM, 04510 México, DF, Mexico

ARTICLE INFO

Article history:
Available online 11 July 2014

Keywords:
Transition metal compounds
X-ray absorption
X-ray emission
Mott–Hubbard insulator
Charge transfer insulator
Oxidation states

ABSTRACT

Direct probe of Mott–Hubbard (MH) to charge-transfer (CT) insulator transition in the MF_2 (M = Cr–Zn) family of compounds was observed by combining F K and M L X-ray emission spectra (XES). This transition is evident as a crossover of the F-2p and M-3d occupied states. By combining F K XES data with F K edge X-ray absorption (XAS) data we directly obtained values for the M-3d Hubbard energy (U_{dd}) and the F-2p to M-3d charge-transfer energy (Δ_{CT}). Our results are in good agreement with the Zaanen–Sawatzky–Allen theory. We also present three examples where X-ray absorption at the transition metal $L_{2,3}$ edges is used to study the oxidation state of various strongly correlated transition metal compounds. The metal oxidation state is obtained by direct comparison with crystal field multiplet calculations. The compounds are CrF_2, members of the $La_{1-x}Sr_xCoO_3$ family, and the MVO_3 (M = La and Y) perovskites.

1. Introduction

Core-level spectroscopies are well established tools to study the electronic structure of transition metal (TM) compounds [1]. X-Ray absorption spectroscopy (XAS) provides information about electronic states in the conduction band [1,2] and X-ray emission gives complementary information about occupied states [1]. In the soft X-ray region the electronic transitions follow electric-dipole selection rules and therefore one probes electronic states with inherent atomic and orbital selectivity. This is particularly useful in the study of strongly correlated TM compounds for which XAS and XES at the metal $L_{2,3}$ edge probe, respectively, the metal 3d conduction and valence bands. The absorption spectra are quite sensitive to the intra-atomic effects, including the TM oxidation state. The TM L_{23} absorption spectra can help to identify the TM oxidation state and ligand to metal charge transfer effects [1]. Also, a comparison of emission at the metal L_α and the ligand K_α lines gives a very good indication of the site- and symmetry-projected states of the valence band [3].

In this paper we review recent work in which we observed the Mott–Hubbard to charge-transfer insulator transition in the MF_2 (M = Cr, Mn, Fe, Co, Ni, Cu) family of 3d-transition metal di-fluorides [3]. We also present three examples in which a combination of XAS and theory is used to determine the TM oxidation state in 3d strongly correlated compounds. The first example deals with a member of the MF_2 family, namely, CrF_2, for which there is still a significant disagreement between a single oxidation state atomic multiplet calculation for the $L_{2,3}$ XAS spectrum and experiment [1,4,5]. In the other two examples we show how X-ray absorption at the $L_{2,3}$ edge can be used to determine the oxidation state of transition metal perovskites which, because of their many interesting properties have attracted widespread interest [6]. There are already examples of determination of transition metal oxidation states in complex samples that is extracted by comparing their X-ray absorption data with reference experimental spectra of controlled oxidation states [7]. There is also work in which several oxidation states of vanadium compounds were determined by comparison with multiplet calculations [8].

In the second example we present XAS results for the $La_{1-x}Sr_xCoO_3$ (x = 0, 0.15, 0.3 and 0.5) perovskite family. This is a very interesting system with promising applications as a catalyst [9]. Its performance is linked to changes in its electronic structure induced by the strontium doping fraction x. The increase of strontium content will in principle increase the oxidation state of Co into an unphysical Co^{4+} [9]. The doping process is usually accompanied by oxygen loss in the compound, which would compensate for this change in the cobalt oxidation state [10]. Therefore, to understand

* Corresponding author. Tel.: +525556224673.
E-mail addresses: jimenez@nucleares.unam.mx, jjimenezmier@gmail.com (J. Jiménez-Mier).

http://dx.doi.org/10.1016/j.elspec.2014.07.002
0368-2048/

the effect of strontium doping in this perovskites, a detailed determination of the cobalt oxidation state is very valuable [10].

In the third example we study the vanadium oxidation state of the MVO_3 (M = La, Y) perovskites. They are both antiferromagnetic Mott insulators in which the nominal vanadium oxidation state is V^{3+}. They are strongly correlated systems that have very interesting properties such as a temperature dependent metal-insulator transition, and both exhibit spin, orbital and charge ordering [11]. Evidence of the presence of V^{3+} and V^{4+} in layered $LaVO_3$ samples has been studied by X-ray absorption at the vanadium L-edge [8], where they found a strong presence of V^{4+} in the bulk.

2. Experiment

Fresh commercially available polycrystalline MF_2 samples (M = Cr–Zn) from Sigma–Aldrich with nominal purity greater than 99.9 % were prepared inside a N_2 flow bag and introduced inside the UHV experimental chamber. The polycrystalline samples of the $La_{1-x}Sr_xCoO_3$ (x = 0, 0.15, 0.3, and 0.5) compounds were prepared by standard solid state reaction [12], using La_2O_3, $SrCO_3$, and Co_2O_3 powders with a purity greater than 99.9% as starting materials. X-ray diffraction (XRD) and X-ray photoelectron spectroscopy (XPS) confirm the formation of the $La_{1-x}Sr_xCoO_3$ structure with inhomogeneous grain size. The morphology and crystal size of the final samples were studied by transmission electron microscopy (TEM) and scanning electron microscopy (SEM) [13]. The MVO_3 (M = La, Y) samples were obtained by reduction of MVO_4 prepared by two different methods: solid state reaction and sol–gel acrylamide polymerization [14,15]. Reduction was achieved by heating the MVO_4 samples to 850 °C under vacuum, in the presence of a metallic Zr rod. The resulting powders were characterized by X-ray diffraction, and their size and morphology were studied by TEM and SEM. The only significant difference between the two samples was that the one prepared by sol–gel reaction presented a more homogeneous distribution of smaller crystals compared with the solid-state sample [14,15].

All X-ray absorption and emission measurements took place at beamline 8.0.1 of The Advanced Light Source in Berkeley [16]. Experimental X-ray absorption spectra were recorded in the total electron yield (TEY) mode. All XAS and XES spectra presented in this work were recorded at room temperature.

3. Crystal field multiplet calculations

Atomic multiplet crystal-field calculations were performed for different ionic species of the transition metal in CrF_2, $La_{1-x}Sr_xCoO_3$ and MVO_3 (M = Y, La).[17,18]. In these calculations an essentially atomic view of the orbitals is considered and it does not take into account their covalent character. They included intra-atomic multiplet and crystal field effects for CrF_2 and also charge transfer effects for the perovskites [17,18]. The X-ray absorption cross sections were then normalized to the number of 3d holes [18]. These are all semi-empirical calculations for which the crystal field parameters and the charge transfer energy were varied until the best agreement between theory and experiment was obtained. The multiplet structure is calculated in terms of the intra-atomic Slater integrals which are reduced from their Hartree–Fock values to take into account some degree of electron-electron correlation [19]. For CrF_2 crystal field effects are given in D_{4h} symmetry by the 10Dq, Ds and Dt parameters [17]. For the perovskites the calculation is in O_h symmetry, and therefore only the $10Dq$ crystal field energy is needed. However, for these compounds we had to include charge transfer effects. The parameters used are the dd Hubbard energy U_{dd}, the 2p-3d core-hole potential U_{pd}, and the ligand-to-metal charge transfer energy Δ_{CT} [17]. Charge transfer effects induces mixing of the $3d^n$ and $3d^{n+1}\underline{L}$ configurations in the transition metal, where $\underline{L}$ represents a configuration with a hole in the ligand 2p band. The calculation gives the energy of all irreducible representation states of the ground ($3d^N$, $3d^{N+1}\underline{L}$) and excited ($2p^5\ 3d^{N+1}$, $2p^5\ 3d^{N+2}\underline{L}$) configurations. It also gives the transition matrix element between corresponding pairs of states in these two groups. For each oxidation state the transition matrix elements are expressed in terms of a single atomic reduced radial transition matrix element, $<2p||r||3d>$. This approximation neglects spin–orbit and orbital relaxation effects in the transition matrix elements.

Table 1
Parameters used in the CrF_2 spectra calculation.

Parameter	Cr^+	Cr^{2+}	Cr^{3+}
10Dq (eV)	0.80	0.85	0.80
Ds (eV)	0	0.17	−0.20
Dt (eV)	0	−0.07	0.20
Coefficient (this work)	0.17	0.35	0.47
Coefficient (spectrum in Ref. [4])	0.24	0.38	0.38

Table 2
Parameters used in the calculation of the $La_{1-x}Sr_xCoO_3$ spectra.

x	0	0.15	0.3	0.5
10Dq (eV)	1.28	1.25	1.20	1.20
Δ_{CT}	4.0	3.7	3.3	3.20

In an early crystal field multiplet calculation for CrF_2, Theil et al. [4] used a rather large value of the Ds parameter while trying to reproduce the broad L_3 and L_2 features in their spectra. By doing this they only achieved fair agreement with their experimental results. Their interpretation was [4] that it is an effect introduced by a Jahn–Teller distortion for this $3d^4$ configuration. This large Ds parameter introduces a change in the expected ordering of the D_{4h} orbitals [4,17]. In the present work, instead, the calculation considered three oxidation states for chromium, namely, Cr^+, Cr^{2+} and Cr^{3+}. The X-ray absorption spectrum was then a superposition of the three spectra. In this fashion much better agreement between experiment and theory for the data of ref. [4] and our data was obtained. In both cases we used the same values of the crystal field parameters. Also, no change in the orbital ordering was found. The values of the crystal field parameters used are given in Table 1. The lifetime broadening (FWHM) was 0.28 eV [20] and the experimental resolution was 0.50 eV.

For the perovskites (MVO_3 and $La_{1-x}Sr_xCoO_3$) the calculation considered the atomic multiplet and crystal field effects in O_h symmetry which only requires the crystal field energy $10Dq$. However, given the presence of oxygen, charge transfer effects now play a major role. Modeling the TM $L_{2,3}$ XAS spectra requires accounting the attracting potential exerted by the 2p core hole on the valence electrons. This is captured by the difference between U_{dd} and U_{pd}, which is usually set to −2 eV for oxides [17]. The charge transfer energy Δ_{CT} and $10Dq$ were varied in each calculation to reach the best agreement with experiment. Three ionic states were used for cobalt, namely Co^{2+}, Co^{3+}, and Co^{4+} and two ionic states were used for vanadium, namely V^{3+} and V^{4+}. The parameters used in the cobalt calculation are shown in Table 2. The lifetime broadening was 0.50 eV and the experimental resolution was 0.50 eV.

For vanadium we performed the calculation in O_h symmetry. For the two families of compounds we only used two values of the crystal field parameter $10Dq$, namely 1.7 eV for V^{3+} and 1.4 eV for V^{4+}. For the two oxidation states, the charge transfer energy was Δ_{CT} = 0.0. The lifetime broadening was 0.25 eV for L_3 and twice this value (0.50 eV) to take into account the large broadening of the L_2 structure introduced by the Coster–Kronig decay of the $2p_{1/2}$ core-hole [21]. The absorption spectra of all four compounds were then

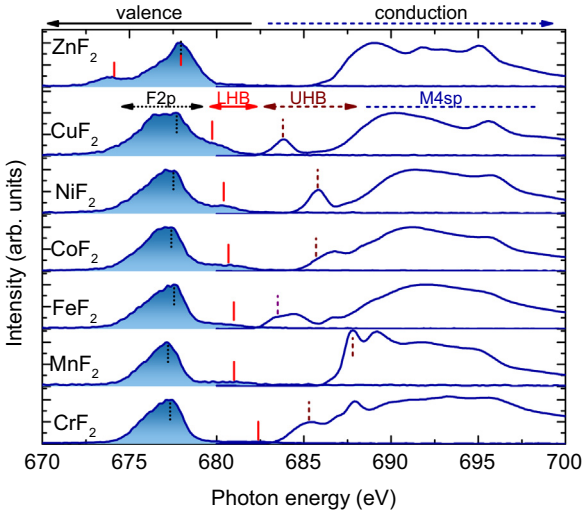

Fig. 1. Fluorine K-edge XAS and XES of the MF_2 family.

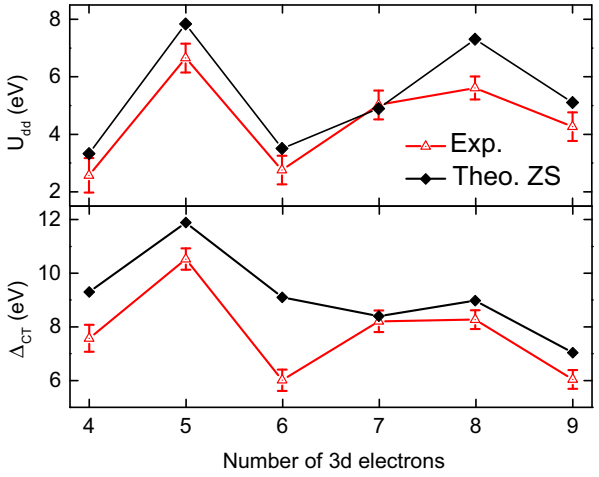

Fig. 2. Comparison between the experimental and theoretical values for the ZSA parameters U_{dd} and Δ_{CT} for the MF_2 family.

reproduced as simple linear combinations of these two calculated spectra.

4. Results

4.1. Mott–Hubbard to charge-transfer transition in the TM di-fluorides

We recently showed that the signature of the evolution from Mott–Hubbard to charge transfer insulator can be found by comparing X-ray absorption and normal emission at the transition metal L and the fluorine K edges [3]. Even for these ionic compounds experiment indicates that at the fluorine absorption and emission spectra there are features that occur because of mixing between the fluorine 2p orbitals and the transition metal 3d orbitals. Plotting the metal L_α and the fluorine K_α normal emission using a common energy scale allows a direct identification of the projected M-3d and F-2p bands in the valence band [3]. Therefore, in the fluorine normal emission spectra one can follow the evolution of the fluorine 2p and transition metal 3d (lower Hubbard – LHB) bands [3]. On the other hand, the fluorine K absorption spectra have broad features common to the entire family which result from mixing of the fluorine 2p and the TM 4sp orbitals. The leading edges, however, are characteristic of each TM, and occur because there is hybridization between the TM 3d band (upper Hubbard band – UHB) and the fluorine 2p unoccupied states [3]. The results of this analysis are presented in Fig. 1, which shows the fluorine-K XAS and XES for the family of difluorides. In the figure we also included spectra for ZnF_2 for comparison. The vertical bars show the position of the F 2p and the LHB in the valence band and the UHB in the conduction band. It is clear that the F 2p valence band does not move in energy as the number of 3d electrons in the metal increases. However, the LHB significantly moves from higher energies in chromium to lower energies, closer to the F 2p band in the later metals, and it appears to the other side of the F 2p peak in ZnF_2. In the absorption spectra the effect of filling the TM 3d subshell is quite apparent [3]. The highest energy for the leading edge occurs for the half filled 3d subshell manganese, and the lowest values are found for chromium, iron and copper. One would expect that these experimental findings be reproduced by calculations that will necessarily include covalency effects, such as the cluster calculations [22]. It is also worth mentioning that we also found transition metal atomic multiplet effects at the leading edges of the fluorine K absorption spectra [5].

By placing on a common energy scale both XAS and XES spectra, we were able to extract [3] the important parameters of the Zaanen–Sawatzky–Allen (ZSA) model, namely the Mott–Hubbard energy U_{dd} and the ligand-to-metal charge transfer energy Δ_{CT} [23]. Because U_{dd} is the energy difference between UHB ($3d^{n+1}$) and the LHB($3d^{n-1}$) and Δ_{CT} is the energy between UHB and the center of the F2p band; by extracting the magnitudes of these energies from our spectra in Fig. 1 we were able to establish a direct comparison with the prediction made by Zaanen and Sawatzky [24]. The results are shown in Fig. 2. There is very good agreement in the general trend of both U_{dd} and Δ_{CT}, even though the theoretical value of Δ_{CT} for iron seems to be too high.

4.2. Oxidation states in transition metal compounds

4.2.1. Chromium disproportionation in CrF_2

Among the transition metal difluorides CrF_2 is the only one whose $L_{2,3}$ absorption spectrum is not satisfactorily reproduced by a single oxidation state atomic multiplet calculation [1,4] In our experimental study of the difluoride absorption spectra we obtained a chromium $L_{2,3}$ TEY spectrum that is slightly different from the one reported by Theil et al. Also, it cannot be reproduced by a single ion atomic multiplet calculation [5]. The TEY spectrum obtained in this work is shown at the bottom panel of Fig. 3 and our digitalization of the spectrum presented by Theil et al. [4] is shown in the top panel. It is clear that the spectra are different mainly because the same broad features have different relative intensities. In Fig. 3 we also show the results of our calculations for both experimental spectra. The curves are the result of the convolution of individual Lorentzian lines at each transition and a Gaussian that gives the overall contribution from the monochromator. This is completely equivalent to using Voigt profiles for each transition, and then adding all their contributions. The calculation gives the three small peaks between 580 and 584 eV that are present in both experimental spectra and that could not be reproduced before [4]. Our calculation indicates that they are part of the crystal field multiplet. To properly reproduce the spectrum we had to include three different oxidation states, Cr^+, Cr^{2+} and Cr^{3+}, in our calculations. We think that their origin is inherent to the synthesis process [25] due to a fundamental disproportionation reaction of the type $2Cr^{2+} \rightarrow Cr^+ + Cr^{3+}$ [5]. The same oxidation states, but with different relative intensities, are also present in the spectrum of ref. [4]. The individual oxidation states, weighted by the superposition

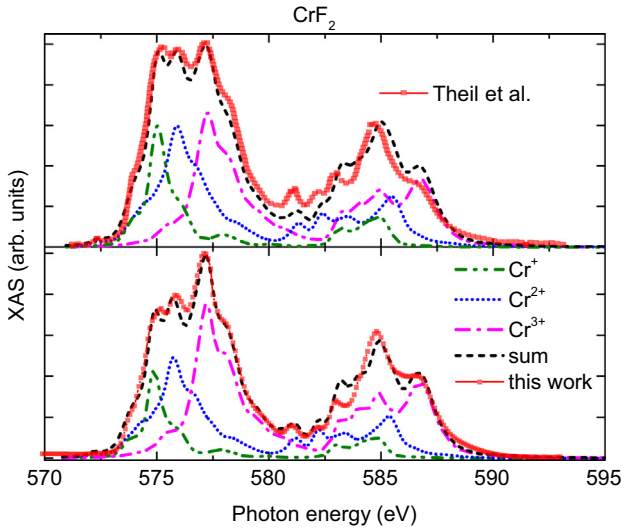

Fig. 3. Comparison between the CrF_2 TEY spectra and the linear combination of calculated Cr^{+}, Cr^{2+} and Cr^{3+} X-ray absorption spectra. Bottom: our data. Top: comparison with the experimental results of Theil et al. [4]. For details see text.

coefficients of each individual calculation, directly give the chromium oxidation state in each sample. This procedure can be applied not only to our sample, but also to the results of Theil et al. [4]. In our sample we have $Cr^{2.26+}$, while in the spectrum of Theil et al. [4] it is $Cr^{2.14+}$. To the best of our knowledge these are the only results supporting this mixed valency assignment for this compound.

4.2.2. Oxidation states in TM perovskites

The XAS spectra at the cobalt $L_{2,3}$ edge of the four members of the $La_{1-x}Sr_xCoO_{3-\delta}$ family ($x = 0$, 0.15, 0.3 and 0.5) are presented in Fig. 4. The position of the shoulders at the L_3 edge establishes a clear distinction between the compounds with low strontium doping ($x = 0$ and 0.15) and the compounds with higher strontium doping. The former have a well defined shoulder on the high energy side, just above 780 eV, while the later have a shoulder on the low energy side, at about 776 eV. In a XAS analysis of the phase transition of the $LaCoO_3$ parent compound, Abbate et al. [26] showed that this behavior is indicative of a change of spin in the ground state of the system. The high energy shoulder belongs to a low-spin t_{2g}^6 configuration, and the low energy shoulder to a high spin $t_{2g}^4 e_g^2$ configuration. Thus, one can conclude that the effect of strontium doping is a change in the spin of the ground state. This change in the ground state spin is apparent in the calculated XAS for Co^{3+}, which is indicated by the dash-dotted lines in Fig. 4. This is a crystal field calculation in O_h symmetry that also considered charge transfer effects. We made a detailed study of the spin cross over [27] value of the 10Dq crystal field parameter as a function of the charge transfer energy Δ_{CT}. The result shows that this family of perovskites always stays in the vicinity of the spin cross-over line [13]. However, the charge transfer calculation with just the Co^{3+} ion is not enough to satisfactorily reproduce the experimental spectra. Therefore we decided to include other cobalt oxidation states, namely, Co^{2+} and Co^{4+} that do not have a low-spin to high-spin transition. The results

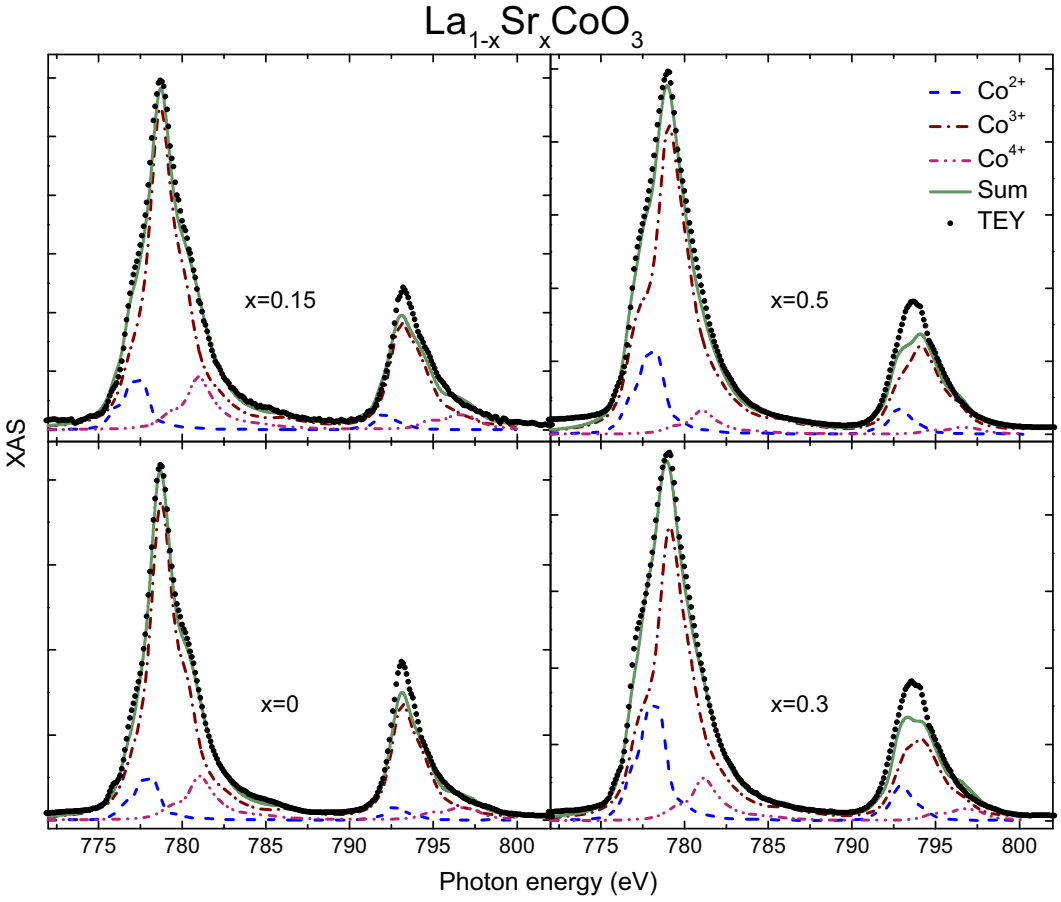

Fig. 4. Comparison between the experimental data and the superposition of calculated Co^{2+}, Co^{3+} and Co^{4+} X-ray absorption spectra for different members of the $La_{1-x}Sr_xCoO_3$ perovskite family.

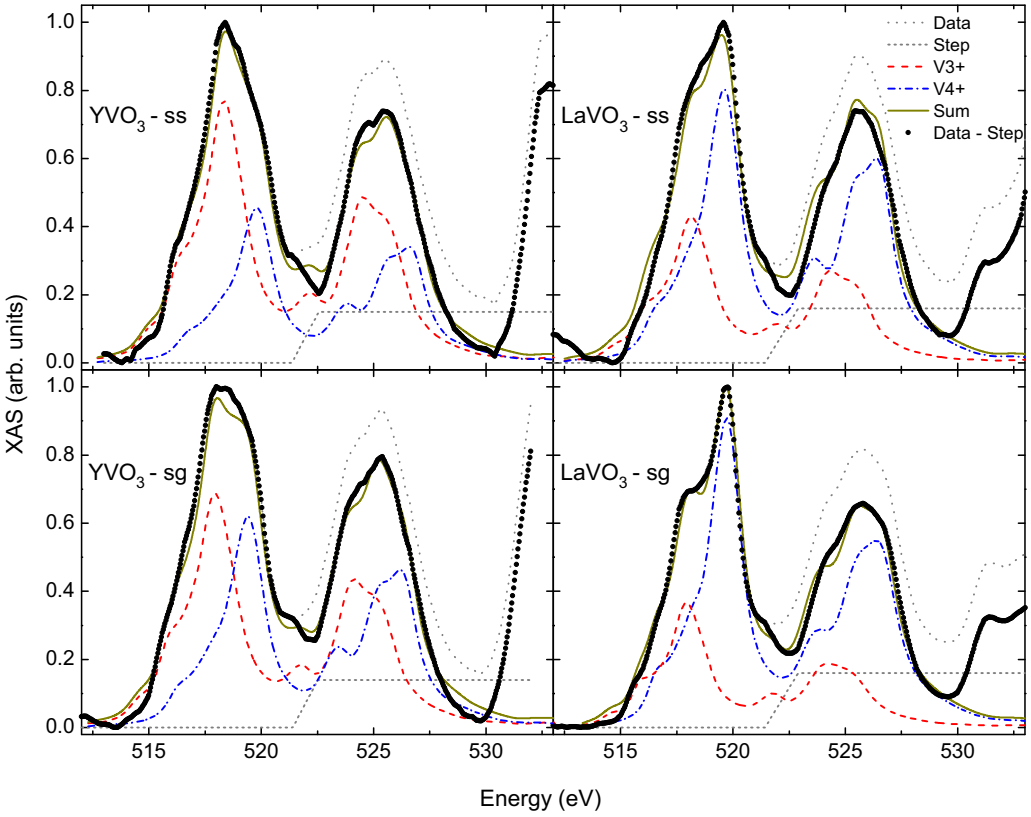

Fig. 5. Comparison between the experimental data and the superposition of calculated V^{3+} and V^{4+} X-ray absorption spectra for the MVO_3 perovskites.

using multiple oxidation states are also shown in Fig. 4. The agreement with experiment is better in the region of the L_3 edge, where all shoulders now have the right height. There is a lower Co^{2+} contribution to the low-spin compounds compared to the high-spin compounds. A significative presence of Co^{2+} in all members of the family is consistent with oxygen loss in the samples.

The final example is a detailed comparison of the XAS of MVO_3 (M = Y, La) samples. The experimental TEY spectra are shown in Fig. 5. Here we have subtracted the L_2 step that is indicated by the dotted line to the experimental data. These spectra show significant broadening in both L_3 and L_2. An atomic multiplet calculation in O_h symmetry for V^{3+} using the values of 10Dq, U_{dd} and Δ_{CT} given by Mossanek et al. [28] does not reproduce any of the spectra. We therefore decided to include the V^{4+} absorption spectrum to improve the fit. Once again, much better agreement between experiment and theory is found by considering linear combinations of these two oxidation states. For YVO_3 the dominant oxidation state is V^{3+} but there is a considerable presence of V^{4+}. There is also a noticeable difference in the ratio of these oxidation states between the two samples. The one prepared with the sol–gel precursor, which has the smaller, more homogeneous crystal size distribution [14] has a larger V^{4+} contribution. In $LaVO_3$ the dominant oxidation state is V^{4+}. A similar behavior for layered structures was found by Wadati et al. [8]. We interpret this change in the oxidation state to chemical effects during the production process by different methods, *i.e.* the presence of large amounts of V^{4+} suggest non-stoichiometric effects caused by excess or deficiency of La or V [8].

Acknowledgements

The Advanced Light Source is supported by DOE (DE-AC03-76sF0009). This work was supported by CONACyT México under research grant No. 56764.

References

[1] F.M.F. de Groot, A. Kotani, Core Level Spectroscopy of Solids, CRC Press, Boca Raton, 2008.
[2] J. Stöhr, NEXAFS Spectroscopy, Springer, Berlin, 1992.
[3] P. Olalde-Velasco, J. Jiménez-Mier, J.D. Denlinger, Z. Hussain, W.L. Yang, Phys. Rev. B 83 (2011) 241102(R).
[4] C. Theil, J. van Elp, F. Folkmann, Phys. Rev. B 59 (1999) 7931–7936.
[5] P. Olalde-Velasco, J. Jiménez-Mier, J. Denlinger, W.-L. Yang, Phys. Rev. B 87 (2013) 245136.
[6] J.B. Goodenough (Ed.), Structure and Bonding, vol. 98, Springer, Berlin, Heidelberg, 2001.
[7] K. Pecher, D. McCubbery, E. Kneedler, J. Rothe, J. Bargar, G. Meigs, L. Cox, K. Nealson, B. Tonner, Geochim. Cosmochim. Acta 67 (2003) 1089.
[8] H. Wadati, D.G. Hawthorn, J. Geck, T.Z. Regier, R.I.R. Blyth, T. Higuchi, Y. Hotta, Y. Hikita, H.Y. Hwang, G.A. Sawatzky, Appl. Phys. Lett. 95 (2009) 023115.
[9] C.H. Kim, G. Qi, K. Dahlberg, W. Li, Science 327 (2010) 1624.
[10] M.A. Se naris Rodríguez, J.B. Goodenough, J. Solid State Chem. 116 (1995) 224.
[11] M. De Raychaudhury, E. Pavarini, O.K. Andersen, Phys. Rev. Lett. 99 (2007) 126402.
[12] G. Thornton, B.C. Tofield, A.W. Hewat, J. Solid State Chem. 61 (1986) 301.
[13] G. Carabalí Sandoval, Caracterización y estudio de la estructura electrónica del sistema $La_{1-x}Sr_xCoO_3$ por medio de la espectroscopia de absorción *y* emisión de rayos *x*, Posgrado en Ciencias Quí micas, UNAM, 2013 (Ph.D. thesis).
[14] G. Herrera, E. Chavira, J. Jiménez-Mier, L. Ba nos, J. Guzmán, C. Flores, J. Sol–Gel Sci. Technol. 46 (2008) 1–10.
[15] G. Herrera, E. Chavira, J. Jiménez-Mier, A. Ordo nez, E. Fregoso-Israel, L. Ba nos, E. Bucio, J. Guzmán, O. Novelo, C. Flores, J. Alloys Compd. 479 (2009) 511–519.
[16] J.J. Jia, T.A. Callcott, J. Yurkas, A.W. Ellis, F.J. Himpsel, G. Samant, J. Stöhr, D.L. Ederer, J.A. Carlisle, E.A. Hudson, L.J. Terminello, D.K. Shuh, R.C.C. Perera, Rev. Sci. Instrum. 66 (1995) 1394.
[17] F. de Groot, Coord. Chem. Rev. 249 (2005) 31–63.
[18] E. Stavitski, F.M.F. de Groot, Micron 41 (2010) 687.
[19] R.D. Cowan, The Theory of Atomic Structure and Spectra, University of California Press, Ltd, Berkeley, 1981.
[20] M.O. Krause, J.H. Oliver, J. Phys. Chem. Ref. Data 8 (1979) 329.
[21] G. Herrera, J. Jiménez-Mier, R. Wilks, A. Moewes, W. Yang, J. Denlinger, J. Mater. Sci. 48 (2013) 6437.
[22] P.S. Bagus, E.S. Ilton, C.J. Nelin, Surf. Sci. Reports 68 (2013) 273.

[23] J. Zaanen, G. Sawatzky, J. Allen, Phys. Rev. Lett. 55 (1985) 418.
[24] J. Zaanen, G.A. Sawatzky, J. Solid State Chem. 88 (1990) 8.
[25] B.J. Sturm, Inorg. Chem. 1 (1962) 665.
[26] M. Abbate, J. Fuggle, A. Fujimori, L. Tjeng, C. Chen, R. Potze, G.A. Sawatzky, H. Eisaki, S. Uchida, Phys. Rev. B 47 (1993) 16124.
[27] J.S. Griffith, The Theory of Transition-Metal Ions, Cambridge University Press, Cambridge, 1961.
[28] R.J.O. Mossanek, M. Abbate, T. Yoshida, A. Fujimori, Y. Yoshida, N. Shirakawa, H. Eisaki, S. Kohno, F.C. Vicentin, Phys. Rev. B 78 (2008) 075103.